PHYSICAL REVIEW E **77**, 065401(R) (2008)

Wake behind dust grains in flowing plasmas with a directed photon flux

W. J. Miloch
Institute of Theoretical Astrophysics, University of Oslo, Box 1029 Blindern, N-0315 Oslo, Norway and School of Physics, The University of Sydney, Sydney, NSW 2006, Australia

S. V. Vladimirov
School of Physics, The University of Sydney, Sydney, NSW 2006, Australia

H. L. Pécseli
Department of Physics, University of Oslo, Box 1048 Blindern, N-0316 Oslo, Norway

J. Trulsen
Institute of Theoretical Astrophysics, University of Oslo, Box 1029 Blindern, N-0315 Oslo, Norway

(Received 15 April 2008; published 24 June 2008)

The wake behind conducting dust grains in a supersonic plasma flow with a directed photon flux is studied by the particle-in-cell method. The electron emission leads to a positive charge on the dust. The resulting plasma wake differs significantly from the case without photoelectrons. This wake is studied for different photon fluxes and different angles between the incoming unidirectional photons and the plasma flow velocity. The simulations are carried out in two spatial dimensions, treating ions and electrons as individual particles.

DOI: 10.1103/PhysRevE.77.065401 PACS number(s): 52.27.Lw, 52.65.Rr

The studies of wakes behind charged objects in flowing plasmas are of general interest for understanding the interactions between charged dust grains in plasmas [1]. Usually, dust grains in plasma devices are charged negatively due to the high mobility of electrons. A characteristic feature, which is due to the plasma flow, is a region of enhanced ion density in the wake [2–6]. The corresponding potential enhancement is considered to be responsible for the alignment of dust grains in a direction of the flow [7–9].

In a space environment, dust grains are exposed to radiation, and therefore photoelectric effects should also be included in the analysis of dust charging [10–13]. Photoemission will change the total charge on the dust and the surface charge distributions and can lead to new types of interactions between dust grains. It was recently shown that the charge of the dust cloud in a plasma discharge can be modified by uv light [14]. Structures comprising positively charged dust grains have already been observed in experiments [15,16].

Despite the relevance of the problem, there are only a few studies on dust charging with photoelectron emission and interactions with the surrounding plasma. In particular, theoretical analyses describe oversimplified models, while experimental studies have limited diagnostics [17–19]. Here, we address this problem by numerical simulations.

We have modified the numerical particle-in-cell (PIC) code used in our previous studies [6,20] by including a photon flux and the photoelectric effect. The code is two-dimensional in Cartesian coordinates for simulations of dust charging in collisionless plasmas. Both electrons and ions are treated as individual particles, with the ion to electron mass ratio being $m_i/m_e=120$, and the electron to ion temperature ratio $T_e/T_i=100$, where $T_e=0.18$ eV. The plasma density is $n=10^{10}$ m^{-2} in the present two-dimensional model. A massive and immobile circular dust grain of radius $r=0.375$ in units of the electron Debye length λ_{De} is placed inside a simulation box of size $50\times 50\ \lambda_{De}$. The dust grain is initially charged only by the collection of electrons and ions. A directed photon flux is switched on after approximately 40 ion plasma periods τ_i. At this time, we can assume that the surface charge distribution has reached a steady state. The code is run typically up to 50 ion plasma periods.

To model a small conductor, the charge is redistributed equally on the dust surface at each time step. Such an algorithm is simple to use and is found in other numerical studies [21], but it does not account for the electric dipole moment on the conducting dust as induced by the anisotropic potential distribution in flowing plasmas. The equally distributed surface charge will not necessarily cancel electric fields inside the dust, and thus the algorithm is not adequate for grains larger than the Debye length or for grains of shapes different from spherical (or circular). An algorithm that enforces constant potential within the dust was used in our previous studies of the charge distribution on larger, complex shaped objects in flowing plasmas [20]. The computational expenses of that algorithm were lengthy simulations and strict constraints on shapes and sizes of simulated dust grains.

In this work, we present results from studies of the influence of the directed photon flux on the dust charging and wake formation in a supersonic plasma flow. Due to the large thermal velocity of electrons, the plasma flow is measured in units of the ion drift velocity v_d, which is set to be $v_d=1.5C_s$, where C_s is the speed of sound. Three different angles between the incoming photons and the direction of the ion drift are considered: $\alpha=\{0°,90°,180°\}$, where $\alpha=0°$ denotes photon flux along the ion flow. The simulated photon flux is taken here to be $\Phi_{h\nu}\in(0.25,2.5)\times 10^{19}$ m^{-2} s^{-1}, which, with photon energies $E_{h\nu}$ of 4.8, 5.5, and 7.2 eV, give photon power densities of $H\in(1.9,28.8)$ W m^{-2}. These photon power densities can be achieved by commercially produced uv lamps (e.g., low-pressure mercury lamps) [22]. The work function W of the dust grain is $W=4.5$ eV, which is

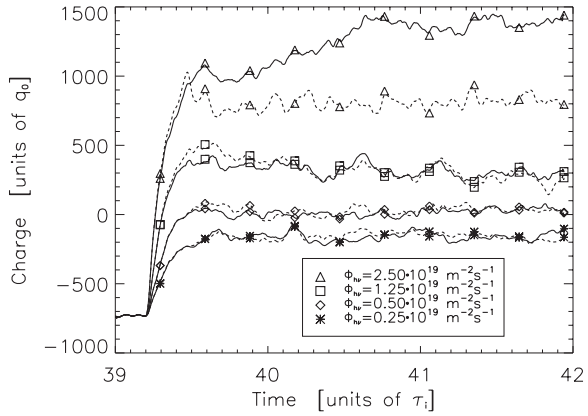

FIG. 1. The total charge q_t on the dust grain as a function of time for different photon fluxes and photon energies. $\alpha=0°$ for all cases. The solid line corresponds to photon energy $E_{h\nu}=5.5$ eV, while the dashed line corresponds to $E_{h\nu}=4.8$ eV. The charge is normalized with the unitary two-dimensional charge $q_0=e[n_{0(3D)}]^{1/3}$, where e is an elementary charge and $n_{0(3D)}$ is the plasma density in the three-dimensional system. The unit of q_0 is $[q_0]=\mathrm{C/m}$. The results are smoothed with the moving box average filter for presentation.

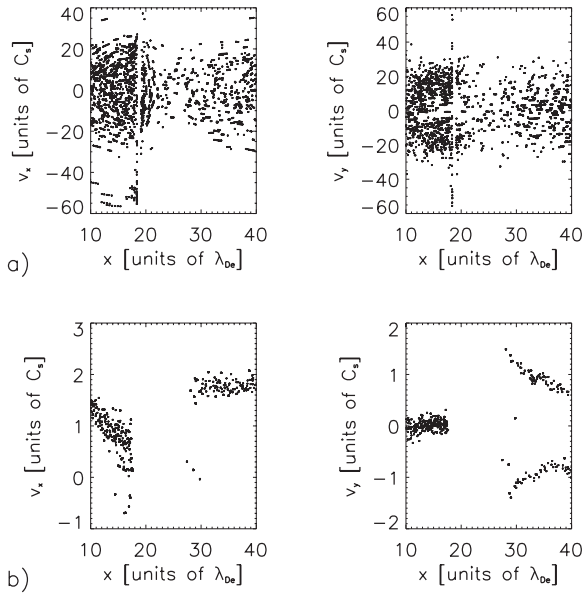

FIG. 2. The x-v_x and x-v_y phase-space plots for electrons (a) and ions (b). The photon energy was $E_{h\nu}=7.2$ eV, and the photon flux $\Phi_{h\nu}=2.5\times10^{19}$ m^{-2} s^{-1} with $\alpha=0°$. The plots correspond to an average over a narrow slice of the simulation box along the x axis of width of $0.25\lambda_{De}$ going through the center of the dust. The center of the dust is at $x=19\lambda_{De}$. We use a narrow slit also in order to have a relatively low phase-space particle density to obtain a transparent presentation.

close to the work functions of many metallic materials [17]. When a photon hits the dust, a photoelectron of energy $E=E_{h\nu}-W$ is produced at distance $l=sv\Delta t$ from the dust surface, where s is a uniform random number $s\in(0,1]$, Δt is the computational time step, and v is the photoelectron speed. Photoelectron velocity vectors are uniformly distributed over an angle of π and directed away from the dust surface.

The charging of dust grains for different photon energies and fluxes is illustrated in Fig. 1. After the onset of the photon flux, the dust charge becomes less negative. It saturates after approximately half an ion period for low photon fluxes and approximately one ion plasma period for large fluxes. The saturation charge is slightly negative for the low photon flux and becomes more positive as the flux increases. For lower fluxes, there is no apparent dependence of the saturation charge on the photon energy, while for higher fluxes, higher photon energy gives rise to a more positive dust charge. The charge fluctuations increase with the photon flux. The relative charge fluctuations are largest for grains with the lowest absolute charge value. The absolute and relative charge fluctuations are smallest for the case without photoemission. We find no dependence of the average charge on the direction of the photons with respect to the ion drift α because of the charge redistribution on the dust surface. For the case of $E_{h\nu}=7.2$ eV, the total charge results are almost identical to the case of $E_{h\nu}=5.5$ eV, and they are therefore not presented here.

The variations of plasma density and potential behind the dust grain depend on the photon flux and photon energy. For low photon fluxes, the total charge on the dust surface is negative and a localized region of enhanced ion density in the wake (ion focusing) is observed. The peak value of the ion density is lower than for the case without the photon flux. The ion focusing characteristic for a negatively charged dust is destroyed when the dust is charged positively. In this case, ions are slowed down in front of the grain and deflected by the dust, which can be inferred from the x-$v_{x,y}$ phase plots shown in Fig. 2. As a consequence, a region of enhanced ion density is formed in front of the dust. When the corresponding ions drift downstream with respect to the dust, they form a distinct boundary between the wake and undisturbed plasma; see also Fig. 3. The shape of the enhanced ion density region depends on the angle between the incoming photons and the ion flow α. It is more pronounced and located closer to the dust surface for $\alpha=0°$, and further from the dust for $\alpha=180°$. For $\alpha=90°$, an asymmetry in the enhanced ion density is observed: the enhancement has a larger spatial extent on the side of the dust where photoelectrons are produced. Slight asymmetries observed for $\alpha=0°$ and 180° are due to the statistical noise in the simulations.

Downstream from the positively charged dust, ions are accelerated toward the wake by the ambipolar electric fields. As a result, a region of strongly reduced ion density is observed. The ion wake, which we refer to as the region where the density is reduced by more than 50% with respect to the undisturbed ion density, scales with the photon flux and photon energy, being larger for higher photon fluxes; see also Table I. It is also larger for photons with higher energies. The ion wake corresponds to the white regions behind the dust grains in Fig. 3.

We note that the ion depletion behind the grain can also be associated with ion absorption on the dust surface [23,24]. Although such an effect is of minor importance for the considered case of supersonic ion drift velocities, it is worth mentioning here since it can lead to the superfluidlike behavior of complex plasmas [25].

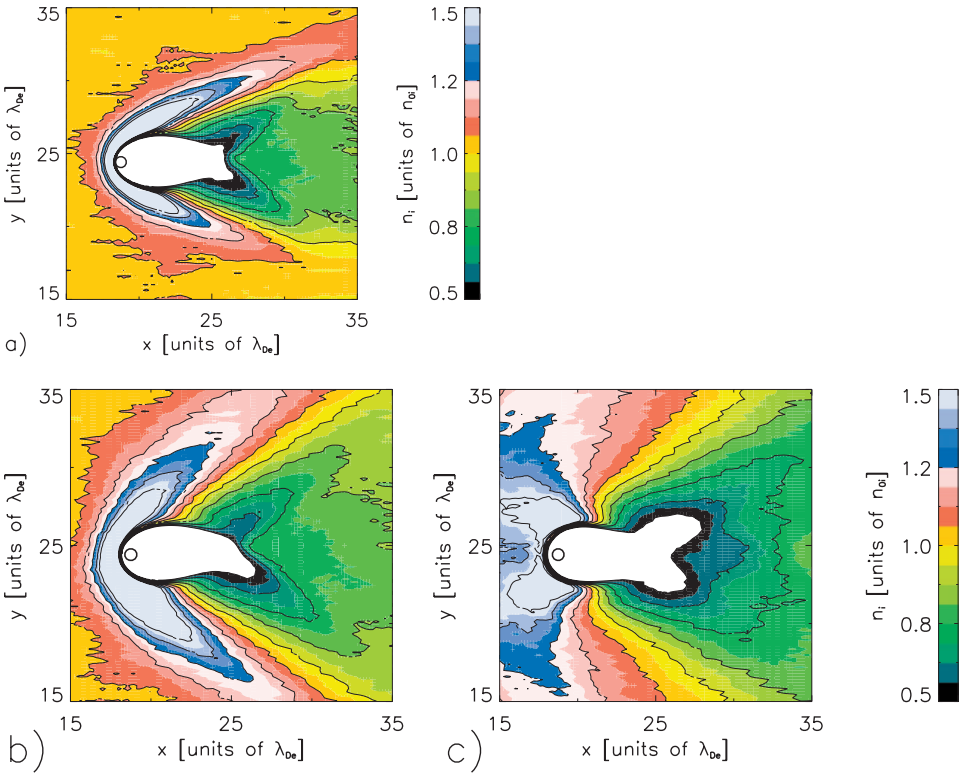

FIG. 3. (Color) The ion density around the dust grain exposed to the photon flux $\Phi_{h\nu}=2.5\times10^{19}$ m^{-2} s^{-1} of energy $E_{h\nu}=4.8$ eV averaged over nine ion plasma periods τ_i for $\alpha=0°$ (a), $\alpha=90°$ (b), and $\alpha=180°$ (c). The plasma flow is in the positive x direction. The white regions behind the dust correspond to ion densities below $0.5n_{0i}$.

The photoemission provides an electron source on the side facing the photon incidence. Photoelectrons localized in the vicinity of the dust surface are attracted by the positively charged dust grain and redistributed to cancel the positive charge region in front of the dust; see also Fig. 2. If the photoelectron energy is lower than or comparable to the electron thermal velocity, the electrons can easily be lost on the dust surface, while electrons with larger energies are more likely to escape. This, together with the photoemission rate, which is proportional to the photon flux, explains the higher positive charge on the dust for higher energetic photons and higher fluxes.

Since photoelectrons are being attracted by the dust grain and the enhanced ion density region in front of the dust, the photon incidence angle α has little effect on the wake pattern behind the dust. It effects, however, the region in front of the dust; see again Fig. 3. The enhanced ion density region is located closer to the dust for photons with $\alpha=0°$, in which case the photoelectrons can partially screen the charge on the dust grain. For $\alpha=180°$, there is no such screening, and photoelectrons need to go through the potential barrier of the dust. The enhanced density region is located at a distance from the dust surface for this case. Further away from the dust, the electrons closely follow the decelerated and scattered ions.

TABLE I. The width w and length d of the ion wake behind positively charged dust grains for different photon energies $E_{h\nu}$ and different photon fluxes $\Phi_{h\nu}$ for $\alpha=0°$. The unit of w and d is the electron Debye length λ_{De}. For $\Phi_{h\nu}<0.5\times10^{19}$ m^{-2} s^{-1}, the dust grains were negatively charged.

	$E_{h\nu}=4.8$ eV		$E_{h\nu}=5.5$ eV		$E_{h\nu}=7.2$ eV	
$\Phi_{h\nu}$ (10^{19} m^{-2} s^{-1})	w (λ_{De})	d (λ_{De})	w (λ_{De})	d (λ_{De})	w (λ_{De})	d (λ_{De})
0.50	0.7	3.1	0.7	3.5	0.9	3.7
1.25	2.1	6.8	2.3	7.5	2.5	7.3
2.50	3.6	7.0	5.9	11.1	6.3	12.7

The electron density is reduced in the region corresponding to the ion wake, but it is still large enough to give rise to the negative potential region behind a positively charged dust; see Fig. 4. This potential enhancement is more pronounced than the one associated with the ion focusing behind the negatively charged grain, and may lead to strong interactions between positively charged grains along the ion flow. The potential in front of the dust depends on the photon incidence angle α. A positive potential region can develop in front of the dust, provided that the local electron density is insufficient to fully neutralize the enhancement in the ion density. In this case, the plasma becomes polarized and can have an associated electric dipole moment. The highest polarization degree is found for $\alpha=180°$. We note again that in our approximation the electric dipole moment on the dust grain itself is assumed to be negligible.

An interesting question is to what degree electrons are Boltzmann-distributed in the vicinity of dust grains. In Fig. 4, we illustrate also the difference δ between the density of Boltzmann-distributed electrons that would correspond to the calculated potential and the actual electron density: $\delta=n_{e0}\exp(-e\Psi/kT_e)-n_e$, where $e<0$ is the electron charge. Before the onset of the photon flux, the electrons can be well approximated by the Boltzmann distribution. With photoemission, the electrons are no longer Boltzmann-distributed. The largest discrepancies are associated with the surplus of

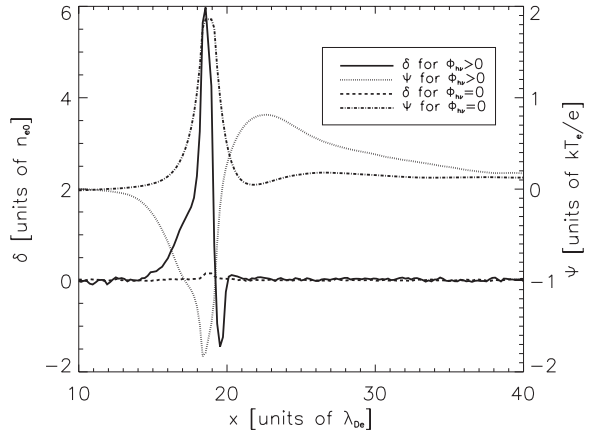

FIG. 4. The potential Ψ profile along the x axis through the center of the dust grain for the case with (dotted line) and without (dash-dotted line) the photoemission. The difference δ between the density of Boltzmann-distributed electrons that would correspond to the calculated potential and the actual electron density is shown for both cases (dashed line, without photoemission; solid line, with photoemission). $\Phi_{h\nu}=2.5\times10^{19}$ m^{-2} s^{-1}, $E_{h\nu}=4.8$ eV, and $\alpha=180°$ for the cases with photoemission.

electrons due to the photoelectron emission, and to the region of the enhanced ion density in front of the dust, where electrons are underrepresented.

To summarize, we have presented numerical results for charging of an individual conducting dust grain in the presence of a directed photon flux in a collisionless, supersonic plasma flow. We showed that uv radiation allows for an accurate control of the charge on a metallic dust grain in plasma devices. By an appropriate selection of the photon flux intensity, coagulation of the small dust grains can be induced due to the large fluctuations in their total charge in the presence of the photon flux. The photoemission should also allow control of the height of a dust grain levitated in the sheath of dc discharges.

Photoelectrons together with the positive dust charge modify and polarize the surrounding plasma. There is a negative potential region in the wake, and a positive potential region in front of the dust, the latter corresponding to the enhancement in the ion density. Such a polarization of plasma can lead to interactions between positively charged grains that are stronger than for the corresponding case with negatively charged dust. Finally, it was shown that with photoemission, the electrons have a non-Boltzmann distribution, which makes relevant theoretical analysis of the problem difficult.

This work was in part supported by the Norwegian Research Council (NFR) and by the Australian Research Council (ARC).

[1] S. V. Vladimirov, K. Ostrikov, and A. A. Samarian, *Physics and Applications of Complex Plasmas* (Imperial College, London, 2005).
[2] K. R. Svenes and J. Trøim, Planet. Space Sci. **42**, 81 (1994).
[3] S. V. Vladimirov and M. Nambu, Phys. Rev. E **52**, R2172 (1995); S. V. Vladimirov and O. Ishihara, Phys. Plasmas **3**, 444 (1996).
[4] F. Melandsø and J. Goree, Phys. Rev. E **52**, 5312 (1995).
[5] A. Melzer, V. A. Schweigert, I. V. Schweigert, A. Homann, S. Peters, and A. Piel, Phys. Rev. E **54**, R46 (1996).
[6] W. J. Miloch, J. Trulsen, and H. L. Pécseli, Phys. Rev. E **77**, 056408 (2008).
[7] S. A. Maiorov, S. V. Vladimirov, and N. F. Cramer, Phys. Rev. E **63**, 017401 (2000).
[8] S. V. Vladimirov, S. A. Maiorov, and N. F. Cramer, Phys. Rev. E **67**, 016407 (2003); **63**, 045401(R) (2001).
[9] G. A. Hebner and M. E. Riley, Phys. Rev. E **69**, 026405 (2004).
[10] M. Horányi, Annu. Rev. Astron. Astrophys. **34**, 383 (1996).
[11] J. C. Weigartner and B. T. Draine, Astrophys. J., Suppl. Ser. **134**, 236 (2001).
[12] O. Ishihara, J. Phys. D **40**, R121 (2007).
[13] B. A. Klumov, S. V. Vladimirov, and G. E. Morfill, JETP Lett. **82**, 632 (2005); **85**, 478 (2007).
[14] V. Land and W. J. Goedheer, IEEE Trans. Plasma Sci. **35**, 280 (2007).
[15] V. E. Fortov *et al.*, JETP **87**, 1087 (1998).
[16] A. A. Samarian and O. S. Vaulina, Phys. Lett. A **278**, 146 (2000).
[17] M. Rosenberg, A. Mendis, and D. P. Sheehan, IEEE Trans. Plasma Sci. **24**, 1422 (1996).
[18] S. A. Khrapak, A. P. Nefedov, O. F. Petrov, and O. S. Vaulina, Phys. Rev. E **59**, 6017 (1999).
[19] K. Ostrikov, M. Y. Yu, and L. Stenflo, IEEE Trans. Plasma Sci. **29**, 175 (2001).
[20] W. J. Miloch, H. L. Pécseli, and J. Trulsen, Nonlinear Processes Geophys. **14**, 587 (2007).
[21] G. Lapenta, Phys. Plasmas **5**, 1442 (1999).
[22] K. F. McDonald, R. D. Curry, and P. J. Hancock, IEEE Trans. Plasma Sci. **30**, 1986 (2002).
[23] M. Chaudhuri, S. A. Khrapak, and G. E. Morfill, Phys. Plasmas **14**, 022102 (2007).
[24] S. A. Khrapak, S. K. Zhdanov, A. V. Ivlev, and G. E. Morfill, J. Appl. Phys. **101**, 033307 (2007).
[25] S. V. Vladimirov, S. A. Khrapak, M. Chaudhuri, and G. E. Morfill, Phys. Rev. Lett. **100**, 055002 (2008).